INTERACTIONS OF PERMEANT CATIONS WITH SODIUM CHANNELS OF SQUID AXON MEMBRANES

DAISUKE YAMAMOTO, JAY Z. YEH, AND TOSHIO NARAHASHI
Department of Pharmacology, Northwestern University Medical School, Chicago, Illinois 60611

ABSTRACT To determine how the permeant cations interact with the sodium channel, the instantaneous current-voltage (*I-V*) relationship, conductance-ion concentration relationship, and cation selectivity of sodium channels were studied with internally perfused, voltage clamped squid giant axons in the presence of different permeant cations in the external solution. In Na-containing media, the instantaneous *I-V* curve was almost linear between +60 and −20 mV, but deviated from the linearity in the direction to decrease the current at more negative potentials. The linearity of instantaneous *I-V* curve extended to more negative potentials with lowering the external Ca concentration. The *I-V* curve in Li solution was almost the same as that in Na solution. The linearity of the *I-V* curve improved in NH_4 solution exhibiting only saturation at −100 mV with no sign of further decrease in current at more negative potentials. Guanidine and formamidine further linearized the instantaneous *I-V* curve. The conductance of the sodium channels as measured from the tail current saturated at high concentrations of permeant cations. The apparent dissociation constants determined from the conductance-ion concentration curve at −60 mV were as follows: Na, 378 mM; Li, 247 mM; NH_4, 174 mM; guanidine, 111 mM; formamidine, 103 mM. The ratio of the test cation permeability to the sodium permeability as measured from the reversal potentials of tail currents varied with the test cation concentration and/or the membrane potential. These observations are incompatible with the independence principle, and can be explained on the basis of the Eyring's rate theory. It is suggested that the slope of the instantaneous *I-V* curve is determined by the relative affinity of permeant cations and blocking ions (Ca) for the binding site in the sodium channel. The ionic selectivity of the channel depends on the energy barrier profile of the channel.

INTRODUCTION

A considerable body of information has recently accumulated to indicate that ion permeation through membrane channels is not a simple diffusion process down the electrochemical gradient but permeant ions interact with the channel while passing through it (Adams et al., 1981; Lewis, 1979; Hille, 1975; Horn and Brodwick,1980; Horn and Patlak, 1980). In sodium channels, for example, the following observations are not compatible with the diffusion theory (or the independence principle): (*a*) channel selectivity varies with the internal ionic concentration (Cahalan and Begenisich, 1976; Begenisich and Cahalan, 1980*a*); (*b*) sodium channel currents saturate at high concentrations of permeant ions (Begenisich and Cahalan, 1980*b*; Yamamoto et al., 1984); and (*c*) small cations such as H^+ and Ca^{++} block the sodium current in a voltage dependent manner (Woodhull, 1973; Taylor et al., 1976; Gilly and Armstrong, 1982; Yamamoto et al., 1984; Stimers et al., 1985). Although there has been no systematic study, some foreign permeant cations seem to have a blocking effect on sodium channels (Hille, 1975).

The aim of this study is to determine how the permeant cations interact with the sodium channel during their permeation. Our experiments show that currents through the sodium channel as carried by Na, Li, NH_4, guanidine, and formamidine all saturate at high ionic concentrations with different apparent dissociation constants. Instantaneous current-voltage (*I-V*) curve has a characteristic shape depending on permeating ion species, and it is suggested that the different shape of the instantaneous *I-V* curve results from various degrees of competition of permeating cations with a binding site in the channel. Modified kinetics of the sodium channel by certain permeant cations is also described.

METHODS

All experiments were performed with giant axons from the squid, *Loligo pealei*, at the Marine Biological Laboratory, Woods Hole, Massachusetts. Axons were isolated, cleaned, and perfused internally using the roller method originally developed by Baker et al. (1961) and improved by Narahashi and Anderson (1967). Potassium-free high sodium artificial sea water was used as the external solution and contained (in millimoles per liter): 600 NaCl and 50 $CaCl_2$, buffered at pH 8.0 with 5 mM HEPES. To observe currents carried by sodium substitutes, NaCl was replaced with LiCl, NH_4Cl, guanidine HCl, or formamidine HCl. For solutions with lower concentrations of permeant cations, tetramethylammonium (TMA) chloride was used as an inert substitute. For experiments in which the external Ca concentration was changed, Na concentration was reduced to 350 mM and the remainder of Na was replaced with an

Dr. Yamamoto's present address is Laboratory of Neurophysiology, Mitsubishi-Kasei Institute of Life Sciences, Machida, Tokyo 194, Japan.

Address reprint requests to Dr. Toshio Narahashi.

appropriate amount of Ca and/or TMA. The internal perfusate for all experiments contained (in millimoles per liter): 250 CsOH, 50 NaF, and 250 glutamic acid, and the pH was adjusted at 7.3 with a phosphate buffer. The osmolarity of the solution was balanced at 1,100 mOsmols by adding sucrose.

To examine the shape of instantaneous current-voltage relations, an axon was exposed to a series of external solutions containing different permeant cation species. Measurements in test solutions were preceded and followed by measurement in TMA solution. This procedure precluded any possible contamination of previously administered permeant cations. Records of the outward sodium channel current were also used to examine the reversibility of the effects of permeant cations on sodium channels.

For the current saturation experiments, an axon was exposed to test solutions containing different concentrations of a given cation species in the order of increasing concentration. After measurements with the highest concentration of test cation, the external solution was switched to the TMA solution until the inward current completely disappeared. The external solution with the lowest concentration of cation under study was readministered to examine the reproducibility. The current amplitude during the prepulse in this measurement was compared with that in the earlier measurement in the same test solution. When the difference between these two measurements was larger than 10%, the data were discarded. Measurements were made with at least three axons for a given cation for the whole range of concentrations (60–600 mM).

The membrane potential and membrane current were recorded with the standard axial wire voltage clamp method. The Pt-plated silver electrode assemblies, used as current measuring and guard external electrodes, were positioned on two sides of the axon as close to the membrane as possible. Both ends of the axon located outside the electrically guarded region of the chamber were suspended in air. Voltage offsets arising from various liquid junction potentials in the measuring system were eliminated for each axon by nulling the potential measured between the internal and external voltage electrodes when the former was placed in a pool containing the internal perfusion solution, which was connected via a 3 M KCl agar bridge to the external solution pool containing the latter electrode (Oxford, 1981). Series resistance compensation of up to 5 Ω cm^2 was employed in all experiments. Membrane currents were sampled at 20 μs per point by a 14 bit analog-to-digital converter on-line with PDP 11/23 computer (Digital Equipment Corp., Marlboro, MA). The digitized data were stored on floppy disks. To subtract the linear portion of capacitative and leakage currents from the records, the *P-P/4* protocol was used (Bezanilla and Armstrong, 1977). The current from four subtraction pulses with an amplitude one-quarter (*P/4*) of that of the test pulse (*P*) was digitally subtracted from the test pulse current. When necessary, currents recorded in the presence of tetrodotoxin (TTX) were used for subtraction. This procedure was necessary when Na was substituted with NH_4, because NH_4 permeates potassium channels (Binstock and Lecar, 1969). All experiments were conducted at a temperature of 9.5–10.5°C.

RESULTS

Instantaneous *I-V* Curves in Na Solutions

Although the instantaneous *I-V* relationship of the squid axon sodium channels was originally reported to be approximately linear (Hodgkin and Huxley, 1952; Chandler and Meves, 1965), recent experiments have revealed a marked rectification (Taylor et al., 1976; Gilly and Armstrong, 1982; Stimers et al., 1985). Figs. 1 *A, B,* and *C* depict examples of sodium currents associated with a depolarizing step followed by a second step to three different membrane potentials (Fig. 1 *D*). There was a large and rapid surge of an inward current upon repolarization of the membrane to the second step. This tail current was produced as a result of a sudden increase in the driving force for sodium while the channel could not shut instantaneously. The sodium tail current decayed rapidly at −80 and −60 mV (Figs. 1 *A* and *B*), indicating the time course of the channel closing at those potentials. At +80 mV, however, the tail current decayed more slowly reflecting primarily inactivation of sodium channels (Fig. 1 *C*). It should be noted that even though the driving force at −80 mV was greater than that at −60 mV, the initial amplitude

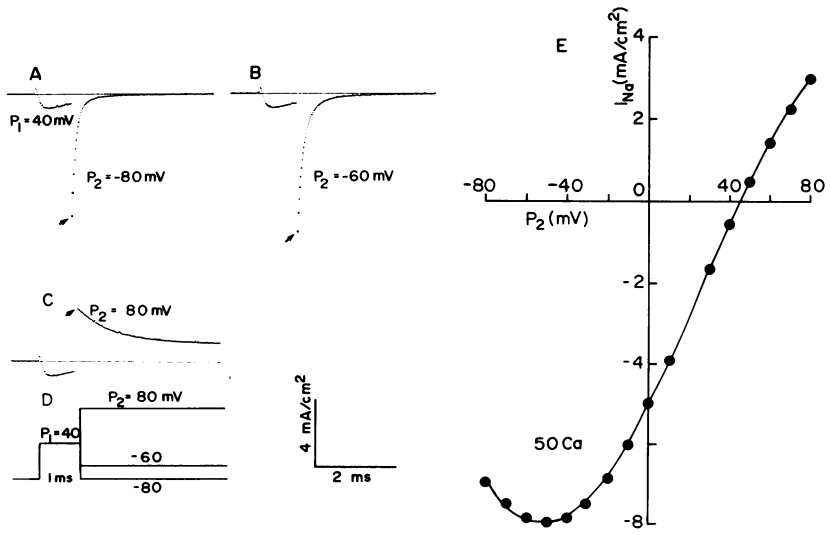

FIGURE 1 Tail currents associated with step repolarization or depolarization (P_2) following a 1 ms conditioning depolarizing pulse (P_1) to +40 mV from a holding potential of −80 mV as shown in the pulse protocol (*D*). *A*, *B*, and *C* show tail currents at P_2 = −80 mV, −60 mV, and +80 mV, respectively. (*E*) Instantaneous current-voltage relationship. The current amplitude at the second digital point (*arrow*) from the beginning of the test pulse is plotted against P_2. Note a marked rectification at large negative potential.

of the tail current at −80 mV was even smaller than that at −60 mV.

To determine the instantaneous current-voltage relationship, the second digital point of the current record during the test pulse was taken as a measure of the amplitude of instantaneous current and was plotted against the membrane potential of the test pulse. The instantaneous *I-V* relation thus obtained exhibits a marked rectification as is shown in Fig. 1 *E*.

The shape of the instantaneous *I-V* curve was drastically changed by changing the external Ca concentration (Fig. 2). In the presence of normal Ca concentration (50 mM), the *I-V* relationship was almost linear at the membrane potentials ranging from +80 to −40 mV (see also Fig. 1 *E*). However, the current deviated from the linearity at more negative membrane potentials, and even decreased with hyperpolarization beyond −80 mV. The deviation from the linearity was more pronounced with increasing the Ca concentration from 50 to 100 mM, and less pronounced with decreasing the Ca concentration to 20 mM. The membrane potential where deviation from the linearity occurred was shifted in the hyperpolarizing direction with decreasing the Ca concentration. The dissociate constants for the Ca block estimated at −60 mV was 156 ± 42 mM (n = 3).

Instantaneous *I-V* Curves in Other Permeant Cations

The instantaneous *I-V* curves recorded from normal axons exposed to five different permeant cations are shown in

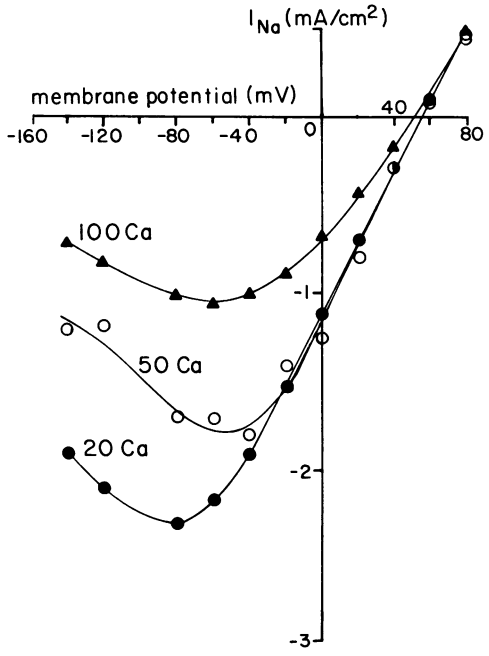

FIGURE 2 Effect of the external Ca concentration on the instantaneous *I-V* relationship of the sodium channel. Three curves were obtained from a single axon in solutions containing 20 mM Ca (●), 50 mM Ca (○), and 100 mM Ca (▲).

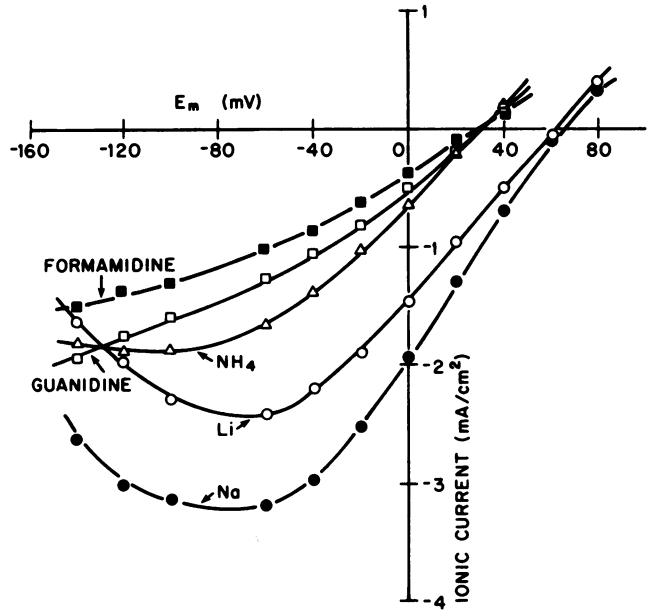

FIGURE 3 Instantaneous *I-V* relationships with various permeant cations. Curves were obtained from different normal axons bathed in a solution containing 600 mM Na (●), Li (○), NH_4 (△), guanidine (□), and formamidine (■).

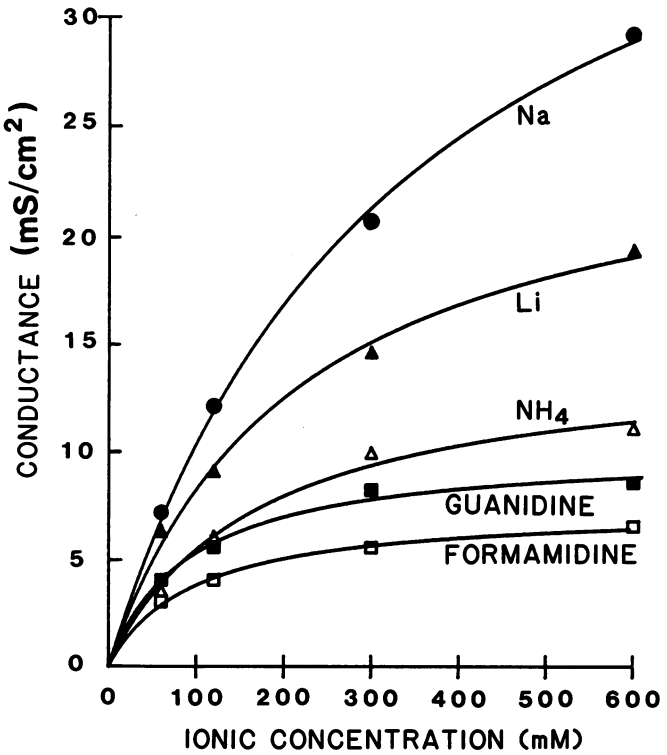

FIGURE 4 Concentration dependence of the channel conductance with various permeant cations. The instantaneous currents were measured when the membrane was repolarized to −60 mV following a 1 ms depolarizing pulse to 0 mV from a holding potential of −80 mV, and the conductances were calculated by Eq. 1. The smooth curves are the least squares fit with rectangular hyperbola. Each curve was obtained with a single axon. The estimated dissociation constants are: 343 mM for Na (●), 215 mM for Li (▲), 168 mM for NH_4 (△), 92 mM for guanidine (■), and 96 mM for formamide (□).

Fig. 3. The *I-V* curves showed two distinct features. First, the shape of *I-V* curves depended on the cation species present externally. The shape of *I-V* curve in Li solution resembled that in Na solution, namely, the *I-V* curve deviated markedly from the linearity at large negative potentials. In contrast, the *I-V* curves in formamidine and guanidine solutions were close to linear. The *I-V* curve in NH_4 solution was intermediate saturating at -100 mV without curving up at large negative potentials. Second, the reversal potential varied depending on the cation species present externally. Na and Li solutions gave a reversal potential of $+64$ mV, whereas formamidine, guanidine and NH_4 solutions gave a reversal potential of $+30$ mV.

Saturation of Sodium Channel Currents

The inward tail currents through sodium channels as carried by Na, Li, NH_4, guanidine, or formamidine ions saturated as the external concentration of these permeant cations was increased. Since changes in the ionic concentration caused the reversal potential to be shifted, the chord conductance rather than the current was used to characterize the saturation of the sodium channel (Takeda et al., 1982). In Fig. 4, the chord conductance in normal axon is plotted as a function of the external permeant cation concentration. The chord conductance for a permeant test cation X (G_X) was calculated by the equation:

$$G_X = I_X / (E - E_X), \tag{1}$$

where I_X is the current amplitude at a membrane potential E, and E_X is the reversal potential for ion X. E was chosen at -60 mV for the measurement of inward tail current for two reasons. First, at -60 mV, the inward current was mainly carried by the external tested ions. Second, the Ca block was not pronounced at this potential.

Plots of G_X vs. concentration are well fitted by a rectangular hyperbola:

$$G_X = G_{X\,max} \cdot [X]/([X] + K_d) \tag{2}$$

where $G_{X\,max}$ is the maximum conductance in test cation, [X] is the external test cation concentration, and K_d is the concentration of ion X that generates 50% of the maximum conductance. The K_d's at -60 mV were estimated to be (mean ± SEM of at least three measurements): Na, 378 ± 34.0 mM; Li, 247 ± 10.0 mM; NH_4, 174 ± 5.3 mM; guanidine, 111 ± 20.9 mM; and formamidine, 103 ± 6.1 mM.

Cation Permeability Ratios

The permeability ratios have been traditionally studied by measuring changes in the reversal potential when one species of ions is replaced by another species. The results of such experiments are illustrated in Fig. 3 in which the reversal potentials measured from the instantaneous *I-V* curves varied in the presence of different permeant cations. The reversal potentials also changed, as expected, with the concentration of permeant cations (Fig. 5). In the presence of sodium, the reversal potential changed 57.5 mV by a 10-fold change in the sodium concentration. This value is very close to that reported by Begenisich and Cahalan (1980*a*) and that predicted by the Nernst equation for sodium, i.e., 56 mV at 10°C. For Li, the shift in the reversal potential was 64.4 mV for a 10-fold change in the concentration. With NH_4, guanidine and formamidine, the shift in the reversal potential was much smaller than that with Na and Li, i.e., 42.5 mV for NH_4, 42.2 mV for guanidine, and 43.6 mV for formamidine for a 10-fold change in the concentration. Begenisich and Cahalan (1980*a*) reported a similar value (41 mV) for internal NH_4 ion but a higher value (53.2 mV) for external NH_4 ion concentration change.

From changes in the reversal potential, the ratio of the test cation permeability (P_X) to the sodium permeability (P_{Na}) was calculated using Eq. 3 derived from the constant field equation (Hodgkin and Katz, 1949).

$$E_X - E_{Na} = \frac{RT}{F} \ln \frac{P_X[X]}{P_{Na}[Na]}. \tag{3}$$

The permeability ratios as a function of the cation concentration are given in Table I (upper half). Guanidine was less permeant than Na, with a P_X/P_{Na} ratio of 0.54 at 60 mM guanidine. The ratio decreased substantially with increasing the guanidine concentration, and reached 0.28 at 600 mM. Ammonium and formamidine showed P_X/P_{Na} ratios of 0.42 and 0.35, respectively, at 60 mM test cation concentration, values slightly smaller than that for guani-

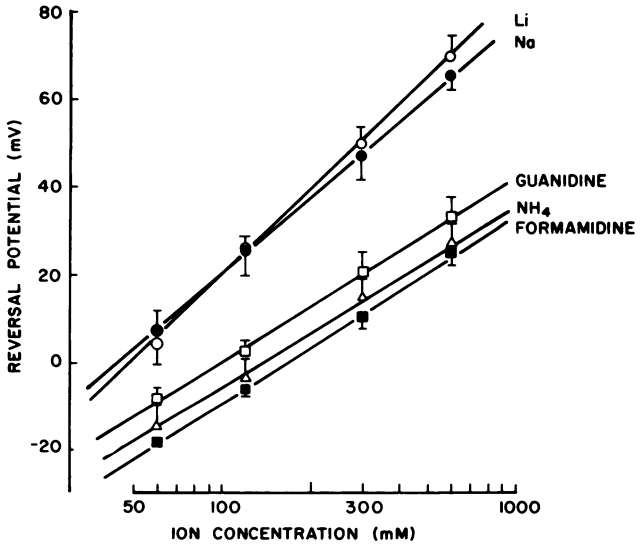

FIGURE 5 Concentration dependence of the reversal potential for tail current with various permeant ions; Na (●), Li (○), NH_4 (△), guanidine (□), and formamidine (■). The reversal potentials were determined by interpolating the instantaneous *I-V* curves. The mean and standard deviation of four measurements are shown, and the straight lines are the least squares fit of data.

TABLE I
PERMEABILITY RATIOS (P_X/P_{Na}) AS A FUNCTION OF THE TEST CATION CONCENTRATION AND OF THE MEMBRANE POTENTIAL IN NORMAL AXONS

Test cation concentration (in millimoles per liter)	Li	NH_4	Guanidine	Formamidine
60	0.90	0.42	0.54	0.35
120	1.02	0.30	0.40	0.28
300	1.13	0.27	0.34	0.23
600	1.19	0.21	0.28	0.20
Membrane potential	**Li**	**NH_4**	**Guanidine**	**Formamidine**
mV				
40	1.09	0.18	0.26	0.16
30	1.04	0.21	0.30	0.18
20	—	0.24	0.33	0.21
10	0.95	0.28	0.39	0.23
0	0.91	0.33	0.45	0.27
−10	0.87	0.38	0.51	0.30

dine. Like guanidine, the P_X/P_{Na} ratio decreased with increasing the test cation concentration. Lithium had almost the same permeability as Na, but unlike the above three test cations, the P_{Li}/P_{Na} ratio tended to increase from a value of 0.90 at 60 mM Li to 1.19 at 600 mM Li. Thus, concentration-dependent selectivity is observed when plots of reversal potential vs. concentration have slopes different from 56 mV per decade concentration change.

Since the reversal potential changes when ionic concentration is changed, the changes in permeability ratio as calculated by Eq. 3 may arise from an effect of membrane potential change (Eisenman and Horn, 1983). Thus the permeability ratio was calculated at the same reversal potential in a test cation solution and in Na solution. When $E_X = E_{Na}$, the constant field equation is simplified to:

$$\frac{P_X}{P_{Na}} = \frac{[Na]}{[X]}. \quad (4)$$

The permeability ratios as a function of the membrane potential are given in Table I (lower half). For guanidine, the P_X/P_{Na} ratio was 0.26 at 40 mV, and increased with hyperpolarization to 0.51 at −10 mV. Ammonium and formamidine had slightly lower P_X/P_{Na} values being 0.18 and 0.16, respectively, at 40 mV, and again the value increased with hyperpolarization. The P_X/P_{Na} ratio for Li was 1.09 at 40 mV and decreased with hyperpolarization.

Permeant Cations and Sodium Channel Kinetics

Kinetics of activation and inactivation of sodium channels were affected to varying extents by different permeant cations. Examples of currents associated with a step depolarization to −20 mV in normal axons are shown in Fig. 6 for various permeant cations. Formamidine and guanidine slowed both activation and inactivation appreciably, whereas Li and NH_4 had only negligible effects. The slowing of the channel kinetics was most significant in guanidine, the time to peak, τ_h and τ_{tail} were increased to 2.95, 2.49, and 1.55 times of those in sodium, respectively.

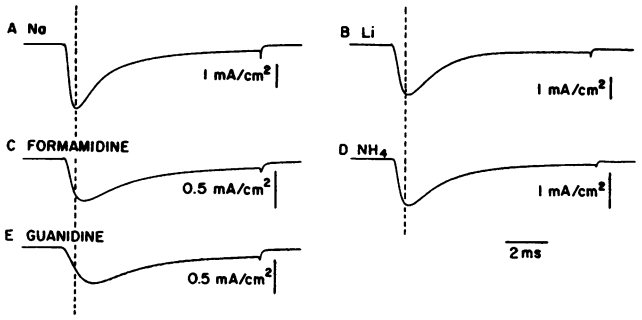

FIGURE 6 Effects of permeant ions on the sodium channel kinetics. Currents were generated by a 10 ms depolarizing step to −20 mV from a holding potential of −80 mV in solutions containing 600 mM Na (*A*), Li (*B*), formamidine (*C*), NH_4 (*D*), and guanidine (*E*). All records were obtained from different axons. The interrupted line is drawn 0.7 ms after the depolarizing step to compare the kinetics in different solutions.

DISCUSSION

The present study demonstrates that the instantaneous *I-V* relationship for the Na current is not linear, but shows a degree of curvature that is intensified with increased Ca ion concentrations (Figs. 1 and 2). This is interpreted as being due to the channel block caused by external Ca ions, which results in a reduced conductance at large negative potentials (Taylor et al., 1976; Gilly and Armstrong, 1982; Mozhayeva et al., 1982; Yamamoto et al., 1984). The new finding reported here is that, in the presence of a constant Ca concentration, the curvature of the instantaneous *I-V* relationship differed depending on the species of permeant cations (Fig. 3). This probably reflects different degrees of competition between the permeant species and the Ca ion for a common site.

To understand the basis for curvature of the instantaneous *I-V* relationships with different ion species, a barrier model (see Yamamoto et al., 1984) based on the Eyring's rate theory was used for computation. This approach treats the channel as a series of energy wells and barriers, and views ion permeation as ions hopping from well to well with a rate that depends on both barrier height and membrane potential. Each internal energy well represents an ion binding site (Hille, 1975; Hille and Schwarz, 1978; Sandblom et al., 1983; Woodbury, 1971). Although the Na channel is considered to be a multi-ion pore (Begenisich and Cahalan, 1980*a*, *b*), the Na channel under physiological condition is approximated as a one-ion pore (Begenisich and Busath, 1981), i.e., multiple simultaneous occupancy is an extremely rare event. Under this assumption the one-ion approximation was applied to the present

analysis. In this model, an ion will cause block, if the ion binds to a site (well) in the channel and cannot hop over energy barrier in the channel.

Preliminary calculations with a four-barrier three-site permeation model (see Yamamoto et al., 1984) indicated that three types of the instantaneous *I-V* curve were possible depending on the depth of the primary energy well. When the primary energy well for a permeant ion is shallower than that for the less permeant blocking ion (e.g., Ca), the instantaneous *I-V* relationship has a negative conductance region at large negative potentials as was seen with Na and Li in our experiments. When the depth of the primary well for a permeant ion is equal to that for Ca, the instantaneous *I-V* curve saturates at large negative potentials without curving upward. With NH_4, this type of instantaneous *I-V* curve was obtained. When the primary well for a permeant ion is deeper than that for Ca, the instantaneous *I-V* curve becomes nearly linear at negative potentials. This was the case for the instantaneous *I-V* curves in formamidine and guanidine solutions. Hence, in the simplified model presented here, the variation of the depth of the outmost (primary) well (while keeping all other barriers/wells constant) will qualitatively describe the spectra of *I-V* relationships in the presence of the various permeant cations.

The depth of the primary energy well can easily be calculated from the apparent dissociation constant K_d using the relation (Hille, 1975):

$$\Delta G = RT \ln K_{d(Em)} \quad (5)$$

where ΔG is the Gibbs free energy (kcal/mol) representing the depth of the primary energy well at the potential *Em*. The apparent dissociation constants for permeant ions were estimated from the conductance-concentration relations (Fig. 4) and that for Ca ion from the Na channel block caused by external Ca ions (Fig. 2). If we assume that the single, identical site is the primary energy well for all of the permeant ions tested and for Ca ion, then we can obtain estimates of the well depth for each ion from experimental K_d values. The ΔG values for various ions are in the following sequence (at −60 mV): Na (−1.0 *RT*) > Li (−1.4 RT) > NH_4 (−1.8 *RT*) > Ca (−1.9 *RT*) guanidine (−2.2 *RT*) = formamidine (−2.3 *RT*).

Similar sequence was obtained by comparing the chord conductance of sodium channel in the presence of various permeant ions. The conductance is the largest in Na solution and smallest in formamidine solution. Fig. 7 illustrates the relationship between the sodium channel conductance in solutions containing different permeant cations and the K_d's of those ions at −60 mV in normal axons. The conductance increases with K_d, namely, an ion with the lowest affinity for the binding site gives rise to the largest conductance. In the Eyring's rate equation the jumping rate of an ion across the barrier is determined by the valley depth as well as the barrier height. As the depth of the energy well increases, the jumping rate decreases.

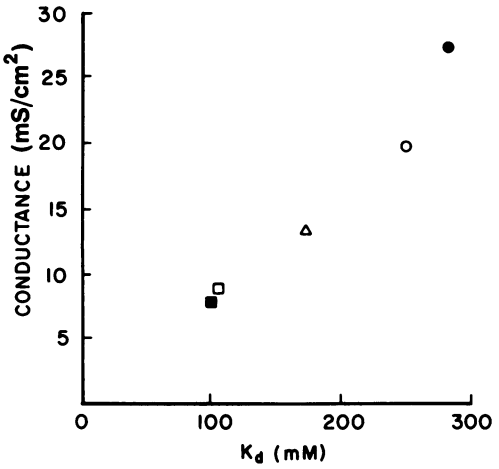

FIGURE 7 Correlation between the channel conductance and apparent dissociation constants for various permeant ions; Na (●), Li (○), NH_4 (△), guanidine (■). Each point is the mean of two to four measurements at a membrane potential of −60 mV in normal axons.

In contrast to the present results for sodium channels, Hoffmann and Dionne (1983) have reported that an increase in affinity of the cation for the acetylcholine-activated channel could result in a larger permeability for the ion. This discrepancy could arise from the difference in location of the binding site in the sodium channel and in the acetylcholine-activated channel. The external primary well in the sodium channel is located 37% in the membrane field as measured from the external surface (Mozhayeva et al., 1982; Yamamoto et al., 1984), whereas the well in the acetylcholine-activated channel is located near the external mouth (Hoffmann and Dionne, 1983). The longer an ion stays in the well, the more likely the ion will go through the channel, because the longer stay will increase the chance for the ion to jump over the barrier (Hoffmann and Dionne, 1983).

The concentration-dependent permeability ratio merits some comments. The concentration-dependent permeability ratio could arise from the effect of changes in the membrane potential or from the occupancy of the wells in the channel (Hille and Schwarz, 1978; Begenisich and Cahalan, 1980*a*; Eisenman and Horn, 1983). It has been shown that for the one-ion pore the reversal potential and the ionic selectivity ratio are more closely related to barrier profiles than the nature of wells (Hille, 1975; Begenisich and Cahalan, 1980*a*). When the barrier heights for different permeant species obey the constant offset energy condition (Hille, 1975), ion permeation through the channel follows the independence principle. Thus the reversal potential changes by changing the ionic concentration with a slope predicted by Nernst equation. If the offset of barrier heights between two ion species is not constant throughout the channel or if the locations of the peak

heights for two ion species are different, the slope of the curve relating the reversal potential to the ionic concentration will deviate from the Nernst's predicted value. The observed slopes of the reversal potential vs. concentration curve with NH_4, guanidine and formamidine were significantly smaller than the Nernst slope (Fig. 5).

However, the potential dependence of the permeability ratio calculated from changes in internal NH_4 ion concentration (Table IV of the paper by Begenisich and Cahalan, 1980*a*) was opposite to that calculated from changes in external NH_4 ion concentrations (Table I of the present results). While this argues against the importance of membrane potential itself in influencing permeability ratio, clearly, the sidedness of NH_4 ion application is critical.

In the multi-ion pore model, the peak heights themselves no longer solely determine the permeability ratio (Hille and Schwarz, 1978), since the occupancy of the wells could affect both the locations and heights of the peaks (Eisenman and Horn, 1983). The opposite potential dependence for change in P_{NH_4}/P_{Na} may be explained by the occupancy of the wells by NH_4 ions. In this model, depolarization would enhance the occupancy of the well by the internal NH_4 ions, and hyperpolarization would also increase the occupancy by external NH_4 ions.

Another interesting observation in this study is that permeant ions alter the gating kinetics of the sodium channel (Fig. 6). Permeant ions have been known to affect gating of acetylcholine-activated channels (Van Helden et al., 1977; Adams et al., 1981; Takeda et al., 1982), voltage activated Ca channels (Saimi et al., 1982; Ashcroft and Stanfield, 1982), and potassium channels (Swenson and Armstrong, 1981). One possible interpretation for this is that any permeant or impermeant ion bound to a site within the channel prevents the gates from closing. It is also possible that a permeant cation interacts with calcium at an external membrane site (Spires, 1985).

We thank Jerry Weiss for computer assistance. This work was supported by grants from the National Institutes of Health (NS14144 and GM24866).

Received for publication 5 October 1984 and in final form 25 March 1985.

REFERENCES

Adams, D. J., W. Nonner, T. M. Dwyer, and B. Hille. 1981. Block of endplate channels by permeant cations in frog skeletal muscle. *J. Gen. Physiol.* 78:593–615.

Ashcroft, F. M., and P. R. Stanfield. 1982. Calcium and potassium currents in muscle fibres of an insect (*Carausius morosus*). *J. Physiol. (Lond.).* 323:93–115.

Baker, P. F., A. L. Hodgkin, and T. I. Shaw, 1961. Replacement of the protoplasm of a giant nerve fibre with artificial solutions. *Nature (Lond.).* 190:885–887.

Begenisich, T. B., and D. Busath. 1981. Sodium flux ratio in voltage-clamped squid giant axons. *J. Gen. Physiol.* 77:489–502.

Begenisich, T. B., and M. D. Cahalan. 1980*a*. Sodium channel permeation in squid axons I: Reversal potential experiments. *J. Physiol. (Lond.).* 307:217–242.

Begenisich, T. B., and M. D. Cahalan. 1980*b*. Sodium channel permeation in squid axons II: Non-independence and current-voltage relations. *J. Physiol. (Lond.).* 307:243–257.

Bezanilla, F., and C. M. Armstrong. 1977. Inactivation of the sodium channel I. Sodium current experiments. *J. Gen. Physiol.* 70:549–566.

Binstock, L., and H. Lecar. 1969. Ammonium ion conductance in the squid giant axon. *J. Gen. Physiol.* 53:342–361.

Cahalan, M. D., and T. B. Begenisich. 1976. Sodium channel selectivity. Dependence on internal permeant ion concentration. *J. Gen. Physiol.* 68:111–125.

Chandler, W. K., and H. Meves. 1965. Voltage clamp experiments on internally perfused giant axons. *J. Physiol. (Lond.).* 180:788–820.

Eisenman, G., and R. Horn. 1983. Ionic selectivity revisited: The role of kinetic and equilibrium process in ion permeation through channels. *J. Membr. Biol.* 76:197–225.

Gilly, W. F., and C. M. Armstrong. 1982. Slowing of sodium channel opening kinetics in squid axon by external zinc. *J. Gen. Physiol.* 79:935–964.

Hille, B. 1975. Ionic selectivity, saturation, and block in sodium channels: A four-barrier model. *J. Gen. Physiol.* 66:535–560.

Hille, B., and W. Schwarz. 1978. Potassium channels as multi-ion single file pores. *J. Gen. Physiol.* 72:409–442.

Hodgkin, A. L., and A. F. Huxley. 1952. The components of membrane conductance in the giant axon of *Loligo*. *J. Physiol. (Lond.).* 116:473–496.

Hodgkin, A. L., and B. Katz. 1949. The effect of sodium ions on the electrical activity of the giant axon of the squid. *J. Physiol. (Lond.).* 108:37–77.

Hoffmann, H. M., and V. E. Dionne. 1983. Temperature dependence of ion permeation at the endplate channel. *J. Gen. Physiol.* 81:687–703.

Horn, R., and M. S. Brodwick. 1980. Acetylcholine-induced current in perfused rat myoballs. *J. Gen. Physiol.* 75:297–321.

Horn, R., and J. Patlak. 1980. Single channel currents from excised patches of muscle membrane. *Proc. Natl. Acad. Sci. USA.* 77:6930–6934.

Lewis, C. A. 1979. Ion-concentration dependence of the reversal potential and the single channel conductance of ion channels at the frog neuromuscular junction. *J. Physiol. (Lond.).* 286:417–445.

Mozhayeva, G. N., A. P. Naumov, and B. I. Khodorov. 1982. Potential-dependent blockage of batrachotoxin-modified sodium channels in frog node of Ranvier by calcium ions. *Gen. Physiol. Biophys.* 1:281–282.

Narahashi, T., and N. C. Anderson. 1967. Mechanism of excitation block by the insecticide allethrin applied externally and internally to squid giant axons. *Toxicol. Appl. Pharmacol.* 10:529–547.

Oxford, G. S. 1981. Some kinetic and steady-state properties of sodium channels after removal of inactivation. *J. Gen. Physiol.* 77:1–22.

Saimi, Y., and C. Kung. 1982. Are ions involved in the gating of calcium channels. *Science (Wash. DC).* 218:153–156.

Sandblom, J., G. Eisenman, and J. Hagglund. 1983. Multioccupancy models for single filing ionic channels: theoretical behavior of a four-site channel with three barriers separating the sites. *J. Membr. Biol.* 71:61–78.

Spires, S. 1985. Sodium channel saturation and alteration of current kinetics by several permeant cations. *Biophys. J.* 47 (2, Pt. 2):437*a*. (Abstr.)

Stimers, J. R., F. Bezanilla, and R. E. Taylor. 1985. Sodium channel activation in the squid giant axon: Steady state properties. *J. Gen. Physiol.* 85:65–82.

Swenson, R. P., and C. M. Armstrong. 1981. K^+ channels close more slowly in the presence of external K^+ and Rb^+. *Nature (Lond.).* 291:427–429.

Takeda, K., P. H. Barry, and P. W. Gage. 1982. Effects of extracellular sodium concentration on null potential, conductance and open time of endplate channels. *Proc. R. Soc. Lond. B. Biol. Sci.* 216:225–251.

Taylor, R. E., C. M. Armstrong, and F. Bezanilla. 1976. Block of sodium channels by external calcium ions. *Biophys. J.* 16 (2, Pt. 2):27*a*. (Abstr.)

Van Helden, D., O. P. Hamill, and P. W. Gage. 1977. Permeant cations alter endplate channel characteristics. *Nature (Lond.).* 269:711–713.

Woodbury, J. W. 1971. Eyring rate theory model of the current-voltage relationship of ion channels in excitable membranes. *In* Chemical Dynamics: Papers in Honor of Henry Eyring. J. Hirschfelder, editor. John Wiley & Sons, Inc., New York. 601–617.

Woodhull, A. N. 1973. Ionic blockage of sodium channels in nerve. *J. Gen. Physiol.* 61:687–708.

Yamamoto, D., J. Z. Yeh, and T. Narahashi. 1984. Voltage-dependent calcium block of normal and tetramethrin-modified single sodium channels. *Biophys. J.* 45:337–344.